Design and Piloted Simulation of a VTOL Flight-Control System

Vernon K. Merrick* and Ronald M. Gerdes†
NASA Ames Research Center, Moffett Field, Calif.

An integrated flight controller, display, and power management system design, suitable for all-weather VTOL flight operations onto small ships, is described. The flight controller decouples the aircraft's translational and attitude motions, which are then commanded by the pilot, through separate controls. A head-up display provides situation and flight director information sufficient to permit zero-zero landings. The system was applied to a VTOL transport model and simulated on moving base simulators at Ames Research Center. Presented herein are results concerning the aircraft's general handling qualities, especially during landings onto a moving ship under Instrument Flight Rules (IFR).

Introduction

THE U.S. Navy has expressed interest in V/STOL aircraft that can operate, in all weather conditions, to and from relatively small ships. One of the most critical and challenging piloting tasks involved in this type of operation is the approach and vertical landing.

The handling qualities problems associated with the task of approach and vertical landing onto a fixed landing pad have been studied during flight tests of the XV-5B[1] and during piloted, moving base simulations of a series of proposed VTOL aircraft.[2-10] In addition, the U.S. Navy sponsored a study of this problem using the X-22A in a series of flight tests during which the first Instrument Flight Rules (IFR) approach and vertical landing were achieved for this class of aircraft.[11]

Recently, an integrated flight controller, display, and power management system was designed for V/STOL aircraft operation in the powered-lift flight regime and tested on the Ames Six-Degree-of-Freedom Simulator (S.01). The principal aim of this work was to provide a pilot with a control and display system that will enable him to fly precise, curved, decelerating approaches to a vertical landing onto a fixed landing pad in IFR (zero-zero) weather conditions.[12] In the process of achieving this aim, an overall evaluation of the fixed-operating-point handling qualities of the selected VTOL transport was made over a range of speeds spanning the powered-lift flight envelope.

Based on the results of the first simulation, the system has now been improved and further tests carried out using the Ames Flight Simulator for Advanced Aircraft (FSAA). These tests were primarily aimed at establishing the effectiveness of the control and display system in an approach and vertical landing task appropriate to naval flight operations onto small ships.

This paper describes the flight controller, displays, and power management system as they currently exist, reviews the results of the first simulation, and presents the latest results derived from the second simulation.

System Description

Flight Controller

A fundamental problem, demonstrated repeatedly in VTOL simulations[5,6] and flight programs,[1,13] is that glide slope and deceleration control, using thrust magnitude and thrust vector angle, are greatly complicated by the inherent control coupling. This point has been highlighted in at least one simulation[8] and in the X-22A flight tests,[11] where significant workload reductions were obtained by giving the pilot uncoupled control of the horizontal and vertical aircraft velocities. This result suggests that, because of the inherent complexity associated with simultaneous control of glide slope and deceleration, important benefits may accrue from removing all undesirable control and basic airframe modal couplings.

A second problem, observed in simulations, is that a need to repeatedly retrim the pitch attitude (which, with some flight controllers, drifts as the airspeed changes) tends to break the pilot's concentration on the primary tracking task and cause a disproportionately large increase in his workload. This result suggests that substantial benefits may accrue from relieving the pilot of as many secondary control tasks as possible.

A third generally observed problem is that, at low airspeeds (30-60 knots), in winds and turbulence, VTOL aircraft tend to develop a random low-frequency motion often described by pilots as "wallowing." The effect is thought to be due to repeated stalling and unstalling of aerodynamic surfaces coupled with low-heave damping.

These problems strongly suggest the need for more powerful flight controllers,[14] and in the case of VTOL aircraft, an extension of flight controller use to translational as well as rotational degrees of freedom. The desirable flight-controller characteristics can be summarized in the following qualitative requirements.

1) Input-output relationship with dynamic characteristics favored by pilots. For most applications these characteristics approximate a second-order system with appropriate frequency and damping.

2) Input-output relationship insensitive to changes of airframe and propulsion characteristics.

3) In the steady-state, commanded variables that are independent of the external disturbances (type 1 servo).

4) Strong gust alleviation.

5) Strong cross-axis decoupling.

The flight-controller concept selected to meet these requirements is shown in Fig. 1. The loop structure differs slightly, depending on whether the commanded variable is a position (Fig. 1a) or a velocity (Fig. 1b). Noteworthy features are the use of an acceleration feedback and the internal loop containing the transfer function $A(s)$, where s is the Laplace transform variable. These two features are largely responsible for the controller's good performance.

The following form was chosen for $A(s)$:

$$A(s) = 1 - \frac{sH_N(s)}{H_D(s)} \frac{h_{D_0}}{h_{N_0}} \prod_{r=1}^{l} (s+p_r) \tag{1}$$

Presented as Paper 77-601 at the AIAA/NASA Ames V/STOL Conference, Palo Alto, Calif., June 6-8, 1977; submitted June 6, 1977; revision received Oct. 6, 1977.

Index categories: Guidance and Control; Handling Qualities, Stability and Control; Simulation.

*Research Engineer, Flight Dynamics and Controls Branch.
†Research Engineer and Pilot, Flight Operations Branch.

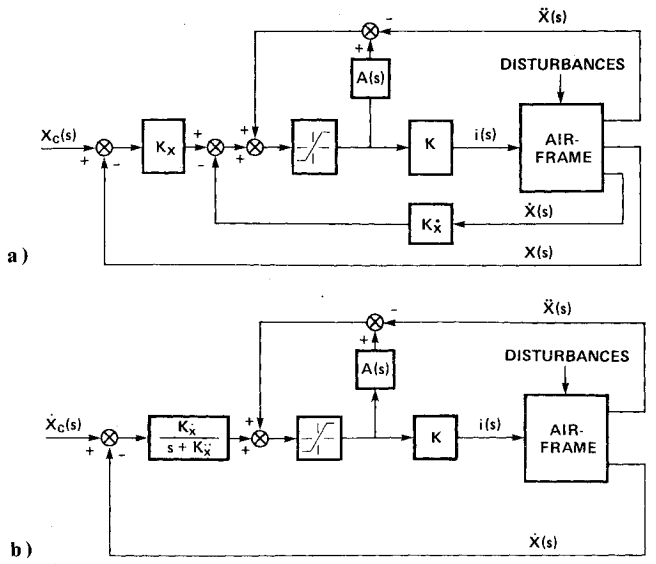

Fig. 1 Single-axis state-rate-feedback-implicit-model-following flight controller. a) position controller, b) velocity controller.

where $H_N(s)/H_D(s)$ is the transfer function of the control actuator in the axis considered; h_{D_0}, h_{N_0} are coefficients of the highest powers of s in $H_N(s)$ and $H_D(s)$, respectively; l is $n-k-l$; n, k are the orders of $H_D(s)$ and $H_N(s)$, respectively; $p_r (r=1 \ldots l)$ are arbitrary numbers open to later selection as poles in the closed-loop root locus; and s is the Laplace transform variable. With $A(s)$ given by Eq. (1), the controller can be made to satisfy the broad requirements given earlier. In particular, it can be shown that[12] if the gain K is sufficiently high, the dynamic behavior of the position-controlled system (Fig. 1a) may be approximated by the second-order equation

$$x_c(s) = [(s^2 + K_{\dot{X}}s + K_X)/K_X]x(s) \qquad (2)$$

whose frequency and damping depend, in a simple way, on the values selected for gains $K_{\dot{X}}$ and K_X. The velocity-controlled system behaves similarly. It follows that the controller is a member of the general class of implicit model-following controllers, and this, together with the use of acceleration (state-rate), has led to the name state-rate-feedback-implicit-model-follower (SRFIMF).

The SRFIMF flight-controller concept was applied to all six degrees of freedom of a comprehensive mathematical model of a lift-fan V/STOL transport.[4,12] The model included thrust lags, flight-control system actuators, and aerodynamic and control system nonlinearities. The aircraft modeled is a six-engine, six-fan V/STOL transport concept based on a DC-9-10. The engine/fan units are interconnected with ducting to permit high-energy gas to flow between pairs of fans, both for attitude control and to prevent large unbalanced moments due to engine failure. Change of forward speed, at a constant pitch angle, is achieved by forward and aft deflection of the thrust vectors of all six fans. At low speed, lateral (translation) control, at constant bank angle, is achieved by lateral deflection of the thrust vectors of all six fans. Pitch and roll control are achieved by differential fan thrust modulation using hot gas "energy transfer and control" (ETaC). At low speeds yaw control is achieved by differential lateral deflection of the thrust vectors of the forward and aft fuselage-mounted fans. The low-speed pitch, roll, and yaw controls are coupled in parallel with the conventional flight-control surfaces. The conventional flight-control surfaces are the same as those on an unmodified DC-9-10, except that the ailerons have been removed and roll control is achieved through wing spoilers.

Table 1 Pilot control modes provided by attitude flight controller (AFC)

SPEED REGIME	ROLL	PITCH	YAW
	STICK	STICK	PEDALS
0-20kt	ROLL ATTITUDE COMMAND	PITCH ATTITUDE COMMAND	YAW RATE COMMAND WITH HEADING HOLD
20-30kt	BLEND		BLEND
30kt-CONVERSION SPEED (120kt)	ROLL RATE COMMAND WITH BANK-ANGLE HOLD		YAW RATE COMMAND WITH BANK-ANGLE FEEDBACK

Table 2 Pilot control modes provided by flight-path flight controller (FPFC)

SPEED REGIME	LONGITUDINAL		LATERAL	VERTICAL
	THUMBWHEEL	THUMB BUTTON	THUMB BUTTON	LEVER
	SLOW, FAST	AFT, FWD	LEFT, RIGHT	DOWN, UP
0-20kt	ACCELERATION COMMAND WITH VELOCITY HOLD	VELOCITY COMMAND	VELOCITY COMMAND	VELOCITY COMMAND
20-30kt		PHASE OUT	PHASE OUT	
30kt-CONVERSION SPEED (120kt)				

It was assumed that any failures of the flight controller would be passive, resulting in the flight controller being automatically disconnected from a basic, unaugmented control system.

A basic philosophy adopted in the application of the controller was that the pitch attitude and horizontal and vertical translational modes of motion should be uncoupled. This decision reflects the opinion of pilots who participated in past NASA simulations. It then becomes convenient to divide the flight controller into two parts: the attitude flight controller (AFC), commanded from the stick (right-hand operation) and pedals, and the flight-path flight controller (FPFC), commanded from the power management console (left-hand operation). The power management console will be discussed in detail later.

The pilot control modes provided by the attitude and flight-path flight controllers are shown in Tables 1 and 2, respectively, and the corresponding control sensitivities and second-order modal characteristics are shown in Tables 3 and 4. The attitude control characteristics are those found to be optimal in Ref. 15. Little information is available from which to select optimum flight-path control characteristics. The values given in Table 4 represent the best guess.

Power Management

A sketch of the power management console is shown in Fig. 2. The power level P and transition lever T directly control the thrust and thrust vector angle, respectively, of all six fans together. The thumb buttom located on top of the power lever (Fig. 2) is a two-axis proportional force transducer by which the pilot can command additional thrust deflections within a 10 deg (semivertex) cone about the nominal thrust deflection (dictated by the T-lever setting). When the FPFC is not in use, this vernier thrust deflection function may be used, in hover, to make small corrections relative to the landing pad just prior to "let-down."

Table 3 Attitude controller characteristics

Axis	Roll	Pitch	Yaw
Pilot's control	Stick	Stick	Pedals
Control sensitivity	Attitude command: 394 deg/m(10 deg/in.)	Attitude command: 175 deg/m(4.44 deg/in.)	Rate command: 485 deg/s/m (12.31 deg/sec/in.)
	Rate command: 263 deg/s/m (6.67 deg/s/in.)	Trim: 4 deg/s	
Control mode frequency rad/s		2.0	
Control mode damping factor		0.75	

Table 4 Flight-path controller characteristics

Axis	Longitudinal		Lateral	Vertical
Pilot's control	Thumb-wheel VC lever	Thumb-button VC lever	Thumb-button VC lever	VC lever
Control sensitivity	Acceleration command: $0.043 m/s^2/deg$ $(0.14 ft/s^2/deg)$		Velocity command: 0.66m/s/N (9.7ft/s/lb)	Velocity command: 80m/s/m (400 ft/min/in.)
Control mode frequency, rad/s			1.25	
Control mode damping factor			0.7	

The velocity control (VC) lever and its associated thumb-operated controls provide the command inputs to the FPFC (Table 2), and are used by the pilot to control vertical velocity (lever) and horizontal acceleration (thumbwheel). The thumb button on top of the VC-lever is similar to that on top of the P-lever, but is coupled into the FPF€ and is used, in hover, to command small horizontal velocities (<20 knots) relative to the landing pad.

In normal operation, with the FPFC switched on, the pilot operates the propulsion system entirely through the VC-lever system. The P- and T-levers are driven by servomotors so that their positions always correspond closely to the power and thrust vector angle required by the FPFC.

If the FPFC either fails or is switched off, the servomotors are automatically stopped and the VC-lever system is electrically disconnected from the FPFC. The pilot then pushes the VC-lever forward through a spring stop at the end of its normal travel (Fig. 2). This action moves the VC-lever out of the pilot's way and declutches the P- and T-levers from their servodrives. The pilot then resumes flight-path control by operating the P- and T-levers manually.

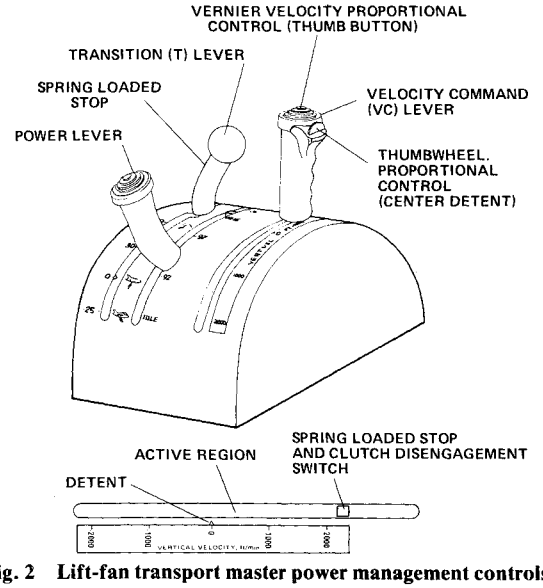

Fig. 2 Lift-fan transport master power management controls.

Displays and Flight Director

The electronic display format is shown in Fig. 3. This display, with some deletions, was projected "head-down" in the first simulation and, in its current form, "head-up" in the second simulation.

The display format is best understood by dividing it into three parts. The attitude display (Fig. 3a) is a typical head-up format which provides the pilot with a complete set of visual attitude cues and corresponding quantitative data. The transition display (Fig. 3b) provides the pilot with guidance during the transition from conversion speed to hover. The left-hand scale (Fig. 3b) indicates longitudinal acceleration in units of ft/s^2; the rightdhand scale indicates vertical velocity in units of 1000 ft/min. Each scale has three pointers: the open arrowhead indicates situation information, the closed arrowhead indicates pilot command information, and the solid bar indicates flight director information. The two scales are used in conjunction with the thumbwheel and VC-lever (Fig. 2 and Table 2). In operation the pilot moves the appropriate control to superimpose the pilot command symbol and flight director symbol. The situation symbol follows the pilot command symbol at the response rate of the aircraft. The terminal display (Fig. 3c) is used to supply guidance from initial hover to touchdown. This part of the display has a combined vertical and horizontal situation format. The landing pad (displayed when the aircraft is within a radius of 152.4 m (500 ft) of the landing pad) is shown in planform, while the deck indicator is shown in vertical aspect. At the initial hover point, the pilot switches to the horizontal velocity command mode operated through the thumb button on the VC-lever (Fig. 2 and Table 2). The commanded and actual horizontal velocity vectors are shown on the terminal display.

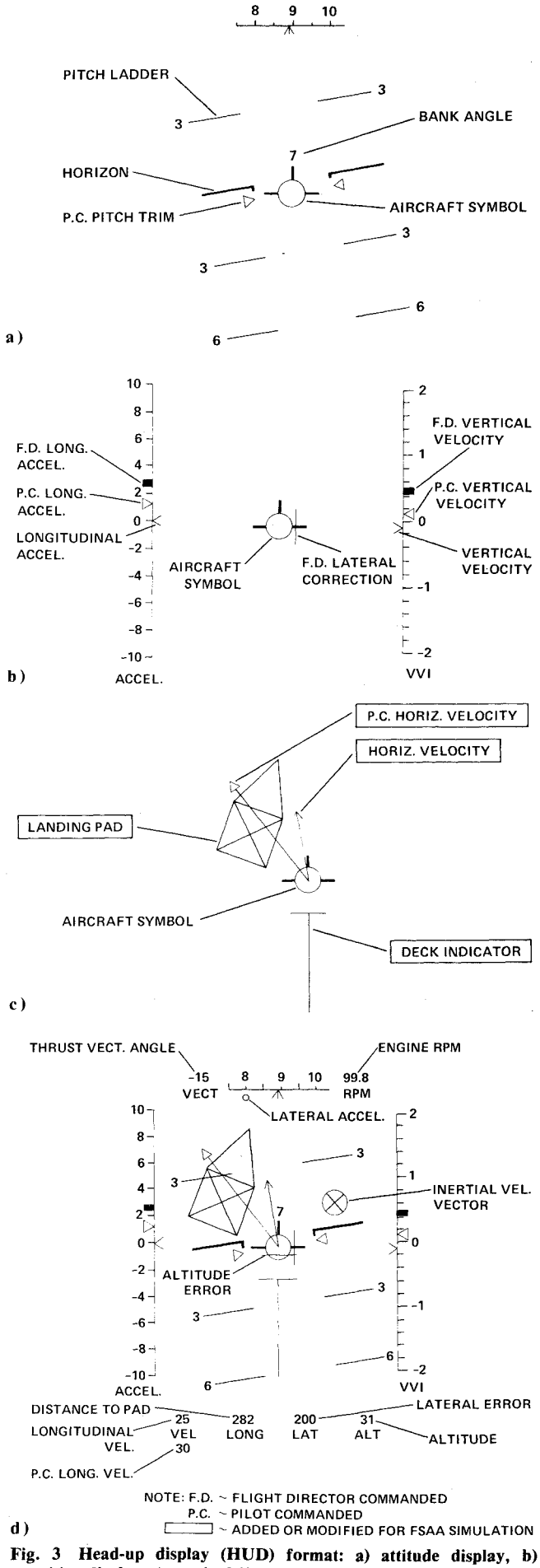

Fig. 3 Head-up display (HUD) format: a) attitude display, b) transition display, c) terminal display, d) complete display.

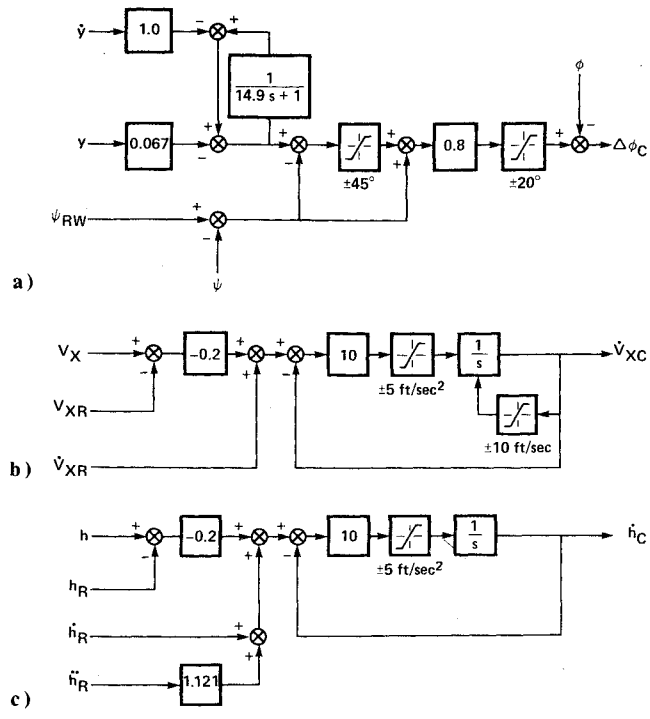

Fig. 4 Flight directors: a) lateral flight director, b) horizontal flight director, c) vertical flight director.

The composite display (Fig. 3d), which is the one viewed by the pilot, contains additional situation.

It should be noted that, where possible, both pilot-commanded and situation information are presented simultaneously. The advantage to this approach is that the pilot is instantly aware of what he has commanded and any discrepancy, in the steady state, between the command and actual values of a variable is a timely indication of a system malfunction. In the event of a flight-controller failure, the pilot command symbols associated with the failed channels become meaningless and are removed from the display to indicate the malfunction.

It is assumed that the desired variation of horizontal and vertical accelerations and velocities along the flight path are known functions of the distance from the touchdown point. Furthermore, it is assumed that both the desired and actual values of these variables are available for use as inputs into a three-axis (lateral, horizontal, and vertical) flight director. Guidance information from the flight director is presented on the display (Fig. 3).

Signal flow diagrams of the three flight directors are shown in Fig. 4. The lateral flight director (Fig. 4a) uses lateral displacement from the localizer y and lateral velocity $\dot{y}$, along with the aircraft and localizer headings ψ and ψ_{RW}, to produce a bank angle command signal $\Delta\phi_C$. The signal $\Delta\phi_C$ is used to drive the short vertical bar shown in Fig. 3b. The horizontal flight director (Fig. 4b) uses aircraft horizontal velocity V_X and the desired horizontal velocity V_{XR} and acceleration $\dot{V}_{XR}$ to produce a horizontal acceleration command $\dot{V}_{XC}$. The signal $\dot{V}_{XC}$ is used to drive the flight-director symbol shown on the left-hand scale of Fig. 3b. The vertical flight director (Fig. 4c) uses aircraft altitude h and the desired altitude h_R, velocity $\dot{h}_R$, and acceleration $\ddot{h}_R$ to produce a vertical velocity command $\dot{h}_C$. The signal $\dot{h}_C$ is used to drive the flight-director symbol shown on the right-hand scale of Fig. 3b. The gain values shown in Fig. 4 are appropriate to input quantities measured in feet, seconds, and degrees.

The flight directors (Fig. 4) are relatively simple and unexceptional. This simplicity is possible because the aircraft, when equipped with the SRFIMF flight controller, has good flying qualities, and additional compensation through the flight directors is not required.

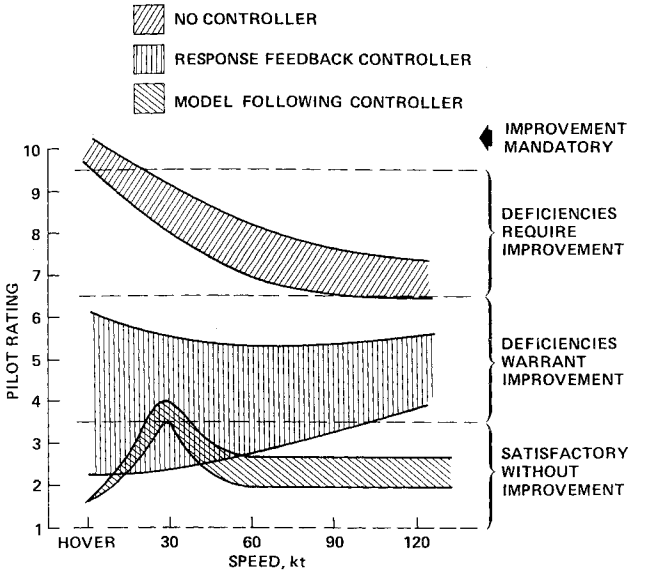

Fig. 5 Fixed-operating-point handling qualities.

Results of First Simulation

Fixed-Operating-Point Handling Qualities

At hover, 30, 60, 90 and 120 knots, the pilot first evaluated the stability and response characteristics of each control mode; then he evaluated the workload involved in performing standard basic maneuvers, such as altitude and velocity changes, steady turns, and sideslips. In addition to rating each small task, the pilot gave an overall opinion rating (Cooper-Harper scale)[16] for the handling qualities at each of the test speeds. The results, shown in Fig. 5, indicate pilot ratings between 1 and 3.5 for the aircraft equipped with the SRFIMF controller. Also shown in Fig. 5 are similar types of results, obtained in previous simulations, for the aircraft without an active controller and for the aircraft with a response-feedback controller. The response-feedback controller referred to here was applied only to the rotational degrees of freedom, used rate and position feedback (no acceleration), and was a type 0 servo (not self-trimming). The aircraft without an active flight controller is clearly unacceptable, while the aircraft with a response-feedback controller, although showing improved handling qualities, has some important deficiencies.

The reason for the somewhat poorer pilot opinion rating (≈ 3.5) in the vicinity of 30 knots, for the aircraft with the SRFIMF controller, is that the yaw controller mode (yaw-rate command with bank-angle feedback) is not entirely satisfactory at low speeds. This particular yaw controller mode is designed so that, above 30 knots, a yaw-rate command signal Δr is fed to the yaw axis for the purpose of coordinating steady banked turns. The yaw-rate command signal is given by

$$\Delta r = (g \tan \phi)/V \qquad (3)$$

where g is the acceleration due to gravity, ϕ is the bank angle, and V is the inertial velocity. In a constant bank-angle turn at constant inertial speed, Eq. (3) shows that Δr is constant. A constant Δr is required to coordinate a steady turn in calm air, but not in the presence of wind. The required variation of Δr to coordinate a steady turn in the presence of a given wind becomes progressively greater with decreasing airspeed. The result of using this type of yaw controller, therefore, is that, at low airspeed, in the presence of wind, large sideslip angles build up in steady, pedal-free turns.

In an attempt to overcome the problem of turn coordination at low speed, an alternate sideslip command mode was tried for the yaw axis. This resulted in excellent turn coordination in calm air and in steady winds, but air turbulence caused high yaw accelerations, which were felt by the pilot as large lateral accelerations. This effect becomes progressively worse with decreasing speed, because the sideslip angles corresponding to a given turbulence level are inversely proportional to speed. At 30 knots with 1.27 m/s (5 ft/s) rms turbulence, the ride quality was unacceptable.

There are many possible solutions to the yaw controller mode problem. For example, it is reasonable to expect that both of the yaw controller modes discussed could be improved; the yaw-rate system by using a filtered airspeed instead of inertial speed in Eq. (3), and the sideslip system by using suitably-filtered sideslip and sideslip rate in its feedback loops.

Except for the yaw controller mode problems. the self-trimming feature of the SRFIMF controller compensated automatically for steady winds, and the disturbance-alleviating properties of the controller greatly attenuated the effects of turbulence. The overall result was that, except for the 30-knot region, winds and turbulence had little effect on the fixed-operating-point handling qualities. Disturbances due to engine failures were likewise quickly removed by the flight controller and required no action from the pilot. The pilot workload involved in dealing with an engine failure received a pilot rating of 1.

Comparison of Two Longitudinal FPFC Modes

Prior to the start of systematic approach and landing tests, the pilot flew several approach transitions to compare the longitudinal FPFC mode shown in Table 1 (longitudinal acceleration command with velocity hold) and an alternate velocity command mode (again using the thumbwheel). To facilitate the use of the velocity command mode, the display (Fig. 3b) was modified by replacing the acceleration scale with a velocity scale.

The major problem observed when using the velocity mode was that the pilot tended to command velocity changes in a series of discrete steps at the frequency of his display scan pattern, rather than smoothly as indicated by the flight director. This step-change technique reduced the tracking accuracy, was a significant workload item, and also reduced the ride quality by introducing large, abrupt, longitudinal decelerations. In contrast, when using the acceleration mode, the pilot found that he needed to apply only one movement of the thumbwheel to establish the deceleration indicated by the flight director. The result was a smooth ride, with high tracking precision, achieved with relatively low workload. The pilot concluded that the acceleration command mode was preferable during transition, at least for the types of constant deceleration approaches flown.

IFR Approaches and Landings to a Fixed Pad

Both straight and curved (in the vertical plane) constant deceleration approaches were flown in the tests. The curved approaches were defined by assuming a constant rate of descent until close to the initial hover altitude. All the approaches were started 4572 m (15,000 ft) from touchdown with the aircraft flying at 120 knots in powered-lift flight. Guidance information was provided down to hover at 6.1 m (20 ft) altitude above the desired touchdown point. The decelerations, initial altitudes, and initial rates of descent for each of the flight paths are shown in Table 5.

All the approaches were started with the aircraft on the glide path, but offset laterally 152.4 m (500 ft) from the localizer and trimmed, nose down, to zero angle of attack. The nose-down attitude was required because the maximum aft thrust vector angle was insufficient for steady unaccelerated flight, with a deck level attitude, at 120 knots, on the steeper approaches (-6 and -9 deg flight-path angle).

The results of the approach and landing tests are shown in Fig. 6. For the straight approaches, the pilot ratings were less than 3.5, independent of the initial approach angle. Sidewinds and turbulence increased the workload slightly, causing the

Table 5 Flight path characteristics

Type	Initial approach angle, deg	Deceleration, m/s^2 (ft/s^2)	Initial altitude, m(ft)	Initial descent rate, m/s(ft/min)
Curved	−3	0.44 (1.45)	460 (1510)	3.20 (630)
	−6	0.85 (2.79)	671 (2200)	6.45 (1270)
	−9	1.19 (3.89)	856 (2810)	9.75 (1920)
Straight	−3	0.91 (3)	244 (800)	3.20 (630)
	−6	0.91 (3)	488 (1600)	6.45 (1270)
	−9	0.91(3)	725 (2380)	9.75 (1920)

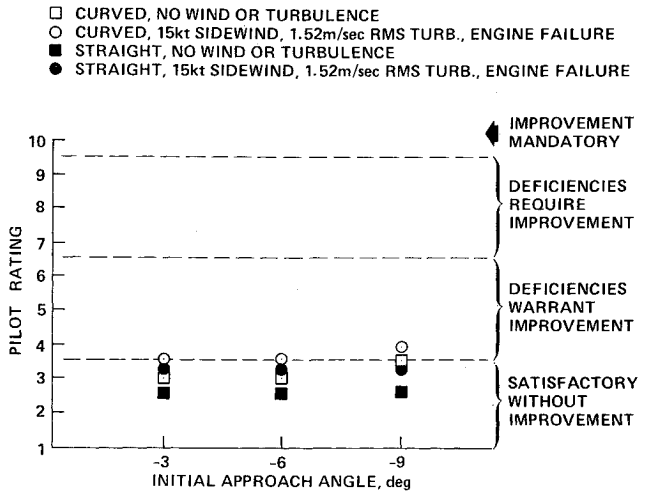

Fig. 6 Lift-fan VTOL approach and landing (IFR zero-zero).

small increase in the pilot ratings shown in Fig. 6. The curved approaches received slightly worse pilot ratings, because the pilot was less comfortable with the higher rates of descent close to the ground. In addition, the curved approaches required more concentration to bring the aircraft to a satisfactory initial hover point.

The greatest operational problem noted was that of switching from the longitudinal acceleration command mode (thumbwheel) to the vernier velocity command mode (thumb button) at the initial hover point. The technique adopted was to watch the commanded velocity indicated on the display (Fig. 3) and, when it reached a value close to zero, to center the thumbwheel and proceed to command velocity with the thumb button. This technique worked reasonably well, but occasionally the pilot centered the thumbwheel when his commanded velocity was not quite zero. This resulted in a residual commanded velocity which had to be constantly countered by using the thumb button. The overall result was increased workload and reduced hovering precision.

The approaches and landings took an average of 30 s longer to perform than the theoretical minimum.[12] This additional time was required because the pilot, rather than follow the vertical flight director all the way to the planned initial hover point, preferred to break off to a hover at about 15.2-30.5 m (50-100 ft) altitude, translate the aircraft horizontally to a position vertically above the landing pad and, finally, descend at about 1.02 m/s (200 ft/min) to touchdown.

FPFC Failure Tests

A series of tests were performed in which FPFC failures were simulated at altitudes varying from 152.4-30.5 m (500-100 ft). Following the failure, the pilot's task was to use the procedure outlined under Power Management to assume flight-path control using the P- and T-levers and abort the landing. In all 10 tests used to evaluate FPFC failures, the pilot was able to check his rate of descent with less than 15.2 m (50 ft) additional loss of altitude; the rate of descent after failure never exceeding that at the failure point. The pilot workload involved in the failure procedure was given a pilot rating of 4.5.

System Modifications Due to First Simulation Results

Flight Controller

As discussed earlier, one of the principal piloting problems involved in the approach and landing task was that of correctly timing the switchover from longitudinal acceleration command (thumbwheel) to longitudinal velocity command (thumb button) for the initial hover. To overcome this difficulty, the flight-controller logic was modified slightly so that, when the pilot pressed the button to select the velocity command mode, the residual commanded velocity, given by the integrated acceleration command, was set at zero. This feature effectively removed any bias from the velocity command mode.

Display

Additions to and modifications of the display are shown in Fig. 3c. The T-shaped deck indicator appears on the display whenever the aircraft is less than 15.2 m (50 ft) above the deck. As the altitude is reduced, the indicator rises to meet the aircraft symbol. (This deck indicator was added because the pilot found it too hard to read the digital altitude indicator and the rate of descent indicator simultaneously.) The deck indicator not only gives a good pictorial indication of both altitude and rate of descent, but also gives these quantities referenced to the actual deck rather than an inertial reference.

To assist the pilot in making precise horizontal position corrections during hover, the commanded and actual velocities in the horizontal plane were added to the display. To move the aircraft to the landing pad quickly and accurately, the pilot presses his thumb button so that his commanded velocity vector passes through the center of the landing pad symbol.

To give the pilot a more representative view of his horizontal situation, the landing pad symbol was modified by adding a point to indicate the bow of a ship, and given rotational freedom to show the relative headings of aircraft and ship.

Results of Second Simulation

Approach and Shipboard Landing Task

The terminal area part of the task is shown pictorially in Fig. 7. The flight paths and deceleration schedules were similar to those used in the first simulation. However, in this instance, flight director guidance was provided to a point 30.5 m (100 ft) aft, 30.5 m (100 ft) to starboard, and 15.2 m (50 ft) above the desired touchdown point. From this initial hover point, the pilot's task was to maneuver the aircraft, in the horizontal plane, to a point vertically above the touchdown point and then descend to touchdown.

The ship, viewed from the initial hover point, is shown in Fig. 7. The full-scale landing area was 18.3 m (60 ft) long and

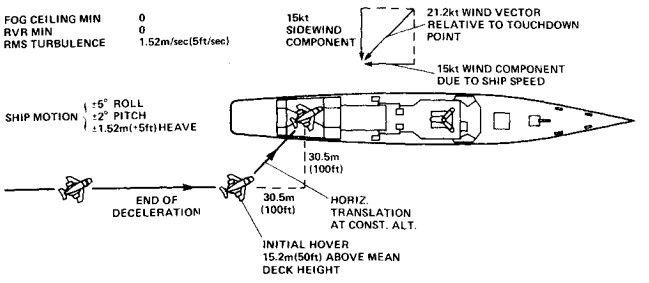

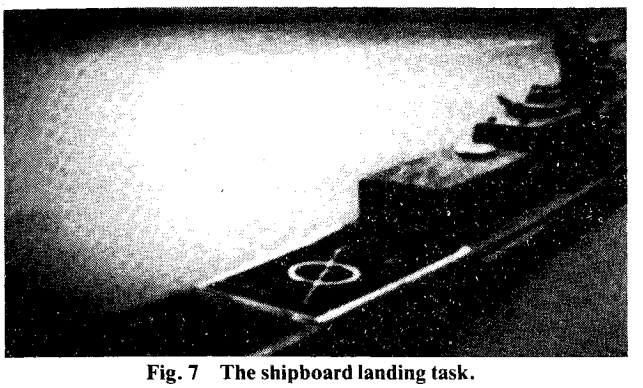

Fig. 7 The shipboard landing task.

15.2 m (50 ft) wide; the touchdown circle was 6.1 m (20 ft) in diam. The roll motion of the ship (ϕ_s) was given by Eq. (4)

$$\phi_s = (A_{sp} + B_{sp} \sin\omega_l t) \sin(\omega_{sp} t + \phi_{sp}) + A_{lp} \sin\omega_{lp} t \quad (4)$$

where ω_{sp} is the short-period frequency, ω_{lp} is the long-period frequency, ω_l is the lull frequency, ϕ_{sp} is the phase angle, A_{sp}, B_{sp}, A_{lp} are the amplitudes, and t is the time. The pitch and heave motions of the ship were given by equations similar to Eq. (4). Equation (4) represents a modulated $(A_{sp} + B_{sp} \sin\omega_l t)$, short-period sine wave $(\sin\omega_{sp} t + \phi_{sp})$ superimposed on a long-period sine wave $(A_{lp} \sin\omega_{lp})$. The maximum and minimum short-period amplitudes are $A_{sp} + B_{sp}$ and A_{sp}, respectively. For this simulation, $\omega_{sp} = 0.4$ rad/s, $\omega_{lp} = 0.015$ rad/s, and $\omega_l = 0.02$ rad/s. The maximum amplitudes of the motion were 5 deg roll, 2 deg pitch, and 1.52 m (5 ft) heave. The "wind-over-deck" was 21.2 knots, comprising a ship speed of 15 knots and sidewind of 15 knots. Turbulence was 1.52 m/s (5 ft/s) rms in all three directions. The conditions for the simulation tests are given in Table 6 along with the corresponding data for the earlier simulation.

Table 6 Approach and landing test conditions

S.01	FSAA
15 knots sidewind	21 knots wind
1.52 m/s(5 ft/s) turb.	1.52 m/s(5 ft/s) turb.
Visibility down to zero-zero	Visibility down to zero-zero
Fixed landing pad	Ship motion ± 5 deg roll, ± 5 deg pitch, ± 1.52m (5 ft) heave
27 landings	17 landings

The aircraft simulated was too large to land on the ship. This problem was overcome by reducing the distance of the pilot forward of the center of gravity from 11 to 4.6 m (36 to 15 ft).

Results

The changes made to the system as a result of the first simulation removed all the problems noted in those tests. Although numerical pilot ratings were not obtained in this simulation, the pilot's assessment of the task and workload indicated an improvement over the previous simulation, even though the shipboard landing task was conceptually more complex than the fixed-pad landing task.

The pilot found the deck and horizontal velocity indicators to be particularly useful during the hover maneuver and letdown. During letdown, the pilot found that he could adjust the rate of descent to match the deck heave motion, and that it was unnecessary to make any attitude adjustment to match the deck attitude. A summary of the touchdown performance obtained during both simulations is shown in Table 7. The mean rate of descent at touchdown was roughly the same for both simulations, even though the landings made in the second simulation were onto a moving deck. The mean touchdown error obtained in the second simulation was half that obtained in the first simulation, due entirely to the removal of any residual velocity after the pilot had finished using the acceleration command mode. The time from initial hover to touchdown was 19 s greater in the second simulation, but this increase occurred because the horizontal location of the initial hover point was displaced 43 m (141 ft) from the touchdown point, rather than directly above the touchdown point as in the first simulation, and because the pilot occasionally required additional time to match his rate of descent to the ship's heave velocity.

To avoid the need for lateral thrust deflection, the velocity command mode in hover was implemented by using aircraft pitch and roll attitudes and was operated through the stick. Results from several landings using this system were compared with those for the velocity command system that used thrust deflection (constant aircraft attitude). Although velocity command through attitude was just as easy as through thrust deflection, and was even more comfortable from a ride viewpoint, the pilots had major reservations about its use. The pilots were not in favor of changing the control function of the stick from attitude command to translational velocity command close to the ground. Apart from the possibility of a system failure, such a scheme means that the pilot must quickly adapt to a different response to stick input in a critical flight condition. In addition, with both the aircraft and ship attitudes changing continuously, the pilots found it hard to judge ship motion, particularly when the horizon was obscured. In contrast, using the thrust deflection technique, the constant attitude of the aircraft provided the pilots with a fixed reference from which to judge ship motion.

Conclusions

An integrated flight controller, displays, and power management system has been advanced as a possible solution to the problem of landing a VTOL aircraft on a small ship in bad weather. Piloted simulations were performed using the

Table 7 Landing performance

	Rate of descent at touchdown, m/s (ft/s)		Touchdown error, m(ft)		Time from initial hover to touchdown, s	
Test	Mean	St. dev.	Mean	St. dev.	Mean	St. dev.
S.01	0.89 (2.91)	0.31 (1.03)	3.94 (12.94)	2.71 (8.88)	30	13
FSAA	1.0 (3.28)	0.34 (1.12)	1.64 (5.38)	0.58 (1.90)	49	10

Ames Six-Degree-of-Freedom Simulator and the Flight Simulator for Advanced Aircraft. The principal conclusions are:

1) The aircraft equipped with the SRFIMF flight controller had satisfactory (PR < 3.5) fixed-operating-point handling qualities throughout the powered-lift flight envelope. These handling qualities were generally better than had been achieved in previous simulations of the aircraft.

2) Some problems still exist with turn coordination at low speeds (< 30 knots). These problems suggest the need for a modified yaw controller mode for speeds greater than 30 knots.

3) With some exceptions related to 2 above, the SRFIMF controller compensated automatically for steady winds, and strongly attenuated the effects of turbulence. The overall result was that winds and turbulence did not materially affect the fixed-operating-point handling qualities.

4) The effects of disturbances introduced by engine failures were quickly and completely removed by the flight controller requiring no action from the pilot.

5) VTOL approaches and landings onto a small ship were flown in 21-knot winds and 1.52 m/s (5 ft/s) turbulence, with ship motion of ±5 deg roll, ±2 deg pitch, and ±1.52 m (±5 ft) heave, and visibility levels down to zero-zero. The pilot workload was rated satisfactory for both curved and straight approaches. However, the pilot had reservations about the desirability of flying the curved approaches because of the high rates of descent close to the deck.

6) For the shipboard landings, the mean rate of descent at touchdown was 1.0 m/s (3.28 ft/s), and the mean touchdown error was 1.64 m (5.38 ft).

7) The features of the power management system and the corresponding procedures aimed at handling the problem of FPFC failures were rated satisfactory.

8) Horizontal velocity command through thrust deflection was preferred over horizontal velocity command through aircraft attitude, although both were satisfactory from a workload viewpoint.

References

[1] Gerdes, R.M. and Hynes, C.S., "Factors Affecting Handling Qualities of a Lift-Fan Aircraft During Steep Terminal Area Approaches," NASA TM X-62,424, 1975.

[2] Abramson, R. and Cambell, J.E. (Rockwell International), "Flight Controls Analysis," *Lift Fan V/STOL Flight Control Systems Development,* Vol. 1, NASA CR-114, 584, 1972.

[3] Rockwell International, "Simulation Experiment," *Lift Fan V/STOL Flight Control Systems Development,* Vol. II, NASA CR-114, 585, 1973.

[4] McDonnell Aircraft Company, "Analytical Study," *Lift Fan V/STOL Transport Control System Investigation, Phase I,* NASA CR-114, 528, 1971.

[5] McDonnell Aircraft Company, "Moving Base Simulation," *Lift Fan V/STOL Transport Control System Investigation, Phase II,* NASA CR-114,529, 1971.

[6] McDonnell Aircraft Company, "Interim Simulation Experiment," *Lift Fan V/STOL Transport Flight Control System Development Continuation,* Vol. I, NASA CR-114,540, 1972.

[7] McDonnell Aircraft Company, "Analytical Studies and Display Development," *Lift Fan V/STOL Transport Flight Control System Development Continuation,* Vol. II, NASA CR-114,643, 1973.

[8] McDonnell Aircraft Company, "Total System Simulation Experiment," *Lift Fan V/STOL Transport Flight Control System Development Continuation,* Vol. III, NASA CR-114,683, 1974.

[9] Eldridge, W.M., Lambregts, A.A., and Spitzer, R.E. (Boeing), "Analysis of Flight Control Systems and Flight Characteristics," *Piloted Simulation of the Boeing R 984-33 V/STOL Research Aircraft,* Vol. I, NASA CR-114,557, 1973.

[10] Eldridge, W.M., Lambregts, A.A., and Spitzer, R.E. (Boeing), "Results of Piloted Simulation," *Piloted Simulation of the Boeing R 984-33 V/STOL Research Aircraft,* Vol. II, NASA CR-114,558, 1973.

[11] Lebacqz, J.V. and Aiken, E.W., "Results of a Flight Investigation of Control-Display Interactions for VTOL Decelerating Descending Instrument Approaches Using the X-22A Aircraft," Eleventh Annual Conference on Manual Control, NASA TM X-62,464, May 1975.

[12] Merrick, V.K., "Study of the Application of an Implicit Model Following Flight Controller to Lift-Fan VTOL Aircraft," NASA TP-1040, 1977.

[13] Holzhauser, C.A., Morello, S.A., Innis, R.C., and Patton, M., Jr., "A Flight Evaluation of a VTOL Jet Transport Under Visual and Simulated Instrument Conditions," NASA TN D-6754, March 1972.

[14] Miller, Jr., K.G. and Deal, P.L., "Moving-Base Visual Simulation Study of Decoupled Controls During Approach and Landing of a STOL Transport Aircraft," NASA TN-D-7790, 1975.

[15] Greif, R.K., Fry, E.B., Gerdes, R.M., and Gossett, T.D., "Effect of Stabilization on VTOL Aircraft in Hovering Flight," NASA TN-D-6900, Aug. 1972.

[16] Cooper, G.E. and Harper Jr., R.P., "The Use of Pilot Ratings in the Evaluation of Aircraft Handling Qualities," NASA TN-D-5153, 1967.